Bull. Mater. Sci. (2021)44:114
https://doi.org/10.1007/s12034-021-02415-4

Thermal conductivity studies on composites of poly(phenylene ether)/polyamide with hollow glass beads (HGB)

ROSHAN JHA[1], JAN MATTHIJSSEN[2] and RADHA KAMALAKARAN[1,*]
[1]SABIC Research and Technology Pvt. Ltd., Chikkadunnasandra, Bengaluru 562125, India
[2]SABIC Innovative Plastics, Plasticslaan 1, Bergen op Zoom 4612PX, The Netherlands
*Author for correspondence (radha.kamalakaran@sabic.com)

MS received 14 May 2020; accepted 10 December 2020

Abstract. Thermally insulating polymer composites are in focus due to the growing industrial demand for sustainable and energy efficient materials. Polymers are intrinsically poor thermal conductors and this property is further enhanced by the addition of insulating fillers in the polymer matrix. Rigid hollow glass beads (HGB) containing polymeric composites are expected to have low thermal conductivities and have additional properties, such as sound proofing, light weight and improved mechanical properties. Four different types of HGB with varying crush strengths, particle size/distributions and densities were evaluated in poly(phenylene ether/polyamide (PPE/PA66) blend to further reduce the blend's intrinsic thermal conductivity. The results showed that the reduction in thermal conductivity was dependent on density and extent of breakage of HGB during processing. Amongst all the evaluated HGB, S38XHS grade of HGB could significantly reduce the thermal conductivity of PPE/PA66 blend.

Keywords. Thermal insulation; hollow glass beads (HGB); PPE/PA66; composite.

1. Introduction

New regulations on having sustainable and energy efficient [1,2] building constructions are leading to a renewed focus on the development of polymer composites with improved thermal insulation properties. The use of thermally insulating composites as building construction material, will retard the flow of heat into and out of the building, thereby retain the room temperature. This will effectively lead to the overall reduced energy consumption for air conditioning of the interiors of the building, depending upon the external environment. These composites, which will form the structural walls of the building, is expected to be not only insulating, but also durable, light-weight and corrosion-resistant. Studies have shown that polymer composites of natural fibres [3–6] are known to result in materials with a combination of properties, such as good thermal insulation, lightness and good mechanicals, and these properties make them ideal for thermal insulation applications. Natural fibre fillers have several attributes, such as low density, good mechanicals, biodegradable, abundant and most importantly, low-cost. These properties, along with life-cycle assessment [7] studies of these composites, make it an ideal choice for making the insulating building material composites. However, the natural fibre is susceptible to absorb moisture [8], hence, the natural fibre-reinforced composites may not be the ideal candidates for high-strength durable components, such as structural walls in the buildings. They may be used in the manufacture of other composite articles, such as flask, food containers, internal parts of automotive and aircraft, where the material have the requirement of light-weight as well as thermally insulating. Several research groups have reported polymer composites with alternate fillers, which are naturally sourced, industrial wastes [9–12], such as fly-ash cynospheres or commercially sourced e.g., hollow glass beads (HGB) and glass fibres [7,13–15]. The trapped gases in most of these fillers are useful in further reduction of the thermal conductivity of the resulting composites. It is well documented that polymeric foams with trapped air/gas bubbles, have reduced thermal conductivities as compared to the neat polymer itself. The addition of mineral fillers further decreases the overall thermal conductivity of the polymer composite. The synergistic effects of gas and mineral fillers in reducing the thermal conductivity of polymer composites are best realized by the incorporation of HGB into the polymer composites. In our studies, unfilled and glass fibre-filled PPE/PA66 resin blends were used as insulation materials that are incorporated into door and window frames to decrease the thermal conductivity [16]. Further reduction in the thermal conductivity of the blend of polyphenylene ether and polyamide was attempted using HGB containing air. PPE/PA66 is a specialty polymer blend having a wide varieties of beneficial properties, such as heat resistance, chemical

Published online: 23 April 2021

resistance, impact strength, hydrolytic and dimensional stability. The objective of current work is to decrease the thermal conductivity of PPE/PA66 blend by using different HGB with varied crush strength, particle size and density.

2. Experimental

2.1 *Materials*

For preparing the composites, PPE/PA66 resin from SABIC and the 3M^{TM} HGB which are essentially composed of soda–lime–borosilicate glass was used. The other physical properties of these K and S series HGB are outlined in the 3M datasheet and the relevant details are summarized in table 1. Here, the HGB with higher densities have higher thermal conductivities and vice-versa. Hence, it is desirable to use the HGB with lower densities, provided they retain their entities or integrity during the compounding and moulding.

2.2 *Sample preparation by compounding and compression moulding*

PPE/PA66 blended resin from SABIC and HGB from 3M were taken for the study. PPE/PA66 resin and HGB were compounded in a twin-screw extruder (L/D $\sim$ 40) under optimized conditions to minimize the breakage of HGB during processing. The optimized processing conditions were the following: temperature: 300°C, screw speed: 150 rpm, throughput: 8–10 kg h^{-1} and torque: 55–60. The HGB fillers were added downstream and screw design used judiciously for just distributive mixing to minimize the breakage. The pellets were dried at 120°C for 5 h in a forced air-circulating oven and injection-moulded into test plaques. All testing was done using pellets or standard ISO test specimens. All test samples were conditioned for 48 h at 23°C before testing. The as-prepared composites had 10 and 20% loading of each grade of the HGB. Owing to the light and fluffy texture of the HGB, it was difficult to load 20% HGB in one instance i.e., K25 grade of HGB. Hence, for each composite, the actual loading was estimated by wt% of glass beads extracted after charring the compounded pellets. For all the formulations, the thermal conductivity was measured on the injection-moulded plaques and breakage of HGB was estimated by charring the plaques and weighing the residue. The extent of breakage was also visualized by imaging the residue by scanning electron microscopy (SEM).

2.3 *Experimental thermal conductivity of PPE/PA66/HGB composites*

The experimental and predicted theoretical thermal conductivities were measured for the as-prepared composites. The experimental thermal conductivity values, expressed in units of watts per Kelvin per metre (W m^{-1} K^{-1}), were measured according to the guarded heat-flow method as described in ASTM E1530-06 using a TCA 446/3 instrument obtained from NETZSCH, USA. A disc measuring 40 mm in diameter and 3.4 mm in thickness was used as a sample for the thermal conductivity measurement. At thermal equilibrium, the Fourier heat flow equation applied to the composite sample becomes

$$R_s = [[T_u - T_m]/Q] - R_{int} \quad (1)$$

R_s = thermal resistance of the test sample; $T_u - T_m$ = the temperature difference between upper and lower plates, in K; Q = heat flux through the test sample; R_{int} = total interface resistance between sample and surface plates.

In this case, the thermal conductivity (λ) of the material, defined by the Fourier's equation for one-dimensional heat conduction as

$$\lambda = d/R_s \quad (2)$$

d = sample thickness in metres and λ = thermal conductivity in W m^{-1} K^{-1}.

The instrument has a heat flow transducer which measures the temperature gradient between the upper surface and lower surface of the composite disc sample. Thus, the thermal resistance, R of sample can be calculated between the upper and lower surfaces. The thermal conductivity of the samples can be calculated using the input value of thickness and taking the known cross-sectional area.

2.4 *Theoretical thermal conductivity of PPE/PA66 /HGB composites*

The predicted or theoretical thermal conductivity was calculated using Lewis and Nielsen semi-theoretical model

Table 1. Details of the commercial HGB used in the present studies.

Grade of HGB	Mean size (μm)	Wall thickness (μm)	Density (g ml^{-1})	Crush strength (psi)	Thermal conductivity (W m^{-1} K^{-1})
S60HS	30	1.31	0.6	18000	0.2
K46	40	1.31	0.46	6000	0.15
S38XHS	40	1.07	0.38	5500	0.127
K25	55	0.95	0.25	750	0.085

given by equation (3), a modified form of the Halpin–Tsai equation for a two-phase system which assumes an isotropic particulate reinforcement [17,18]. The equation also takes into consideration the shape of the particle as well as its orientation. For spherical fillers, the equation for thermal conductivity of the composite is as follows:

$$\lambda_c = \lambda_m\left[1 + ABV_{gb}\right]/\left(1 - B\psi V_{gb}\right), \quad (3)$$

$$B = \left[(\lambda_{gb}/\lambda_m) - 1\right]/\left[(\lambda_{gb}/\lambda_m) + A\right], \quad (4)$$

$$\psi = 1 + \left[(1 - \phi)/\phi^2\right]V_{gb}, \quad (5)$$

where λ_c = thermal conductivity of the composite; λ_m = thermal conductivity of the matrix; λ_{gb} = thermal conductivity of the glass beads; V_{gb} = volume fraction of the glass beads; A = 1.5 for spherical particles; ϕ = packing factor for glass beads i.e., 0.63.

This model is applicable to predict the thermal conductivity of studied heterophase polymer compositions (PPE/PA66 blend and HGB), since there is huge difference in the thermal conductivities of the individual components.

2.5 *Density measurements of PPE/PA66 /HGB composites*

The efficacy of the as-prepared composite, being thermally insulating material, is largely dependent on retaining the integrity of the HGB during compounding and moulding processes. To get an estimate on the breakage of the HGB in the composite, during the processing stages, density measurements were made. Density (in units of grams/millilitre) was measured on compounded pellet as well as moulded parts by gas pycnometer. Density difference, which is the difference in experimental density measured by gas pycnometer and theoretical density, is a proportional to the breakage of HGB. In the theoretical density measurement, it was presumed that the HGB remain intact during the compounding and moulding processes. Theoretical density was calculated by the mixture rule according to the equation

$$\rho_{composite} = V_{HGB} \times \rho_{HGB} + V_{matrix} \times \rho_{matrix}, \quad (6)$$

where $\rho_{composite}$ is the density of the composite, V_{HGB} is the volume fraction of the HGB, ρ_{HGB} is the density of the HGB, V_{matrix} is volume fraction of the polymeric matrix and ρ_{matrix} is the density of the polymeric matrix.

2.6 *SEM of PPE/PA66 /HGB composites*

To get a qualitative understanding of the breakage of the HGB during the compounding and moulding processes, the pellets and moulded plaques were studied by SEM. The pellets and moulded parts were charred at 550°C for 12 h. The residual ash samples were taken and dispersed on a SEM stub to study the HGB morphology. The distributed residual samples with the SEM stub were coated with gold to make them electron-conductive. The coated samples were inserted in SEM (FEI Quanta 400) and imaged at different magnifications in back-scattered mode.

3. Results and discussion

The compounded pellets and injection-moulded plaques were tested for density differences. It is understandable that if the HGB did not break during these processes, the measured densities would be close to the calculated values. However, HGB were susceptible to breakage during high shear processing and the extent of the breakage was quantitatively estimated by calculating the density changes in the pellet and plaques. Table 2 shows the summarized details of the density calculation, theoretical ρ_T and experimental ρ_E for both pellets and plaques. The suffix '1' is used for pellet samples and '2' for the moulded plaques. The theoretical densities were calculated using equation (6) and the experimental values were obtained using a pycnometer.

Table 2. Estimation of density differences in the pellets and moulded plaques due to HGB breakage.

Sample	HGB loading (wt%)	% char (actual wt% of HGB)	Pellet			Plaque		
			ρ_{E1}	ρ_{T1}	$\rho_{pellet\ (diff)}$ $(\rho_{E1} - \rho_{T1})$	ρ_{E2}	ρ_{T2}	$\rho_{plaque\ (diff)}$ $(\rho_{E2} - \rho_{T2})$
S60HS-10	10	9.6	1.026	1.026	0	1.053	1.026	0.027
S60HS-20	20	18.7	0.976	0.977	0.001	1.006	0.977	0.029
K46-10	10	9.6	1.005	0.982	0.023	1.033	0.982	0.051
K46-20	20	18.2	0.937	0.885	0.052	1.056	0.885	0.171
S38XHS-10	10	7.7	1.002	0.93	0.072	1.017	0.93	0.087
S38XHS-20	20	16.2	0.896	0.813	0.096	0.928	0.813	0.115
K25-10	20	9.4	1.047	0.916	0.131	1.079	0.916	0.163

These values for the pellets and plaques gave the density difference due to breakage. The $\rho_{\text{pellet (diff)}}$ and the $\rho_{\text{plaque (diff)}}$ values are density differences (theoretical-experimental values) seen in the compounded pellets and moulded plaques, respectively (figure 1).

The light and fluffy nature of the HGB makes it challenging to feed in the intended wt%. Hence, in all the theoretical calculations, the actual loading (% char) was considered and not the intended values of 10 or 20%. This is indicated in table 2.

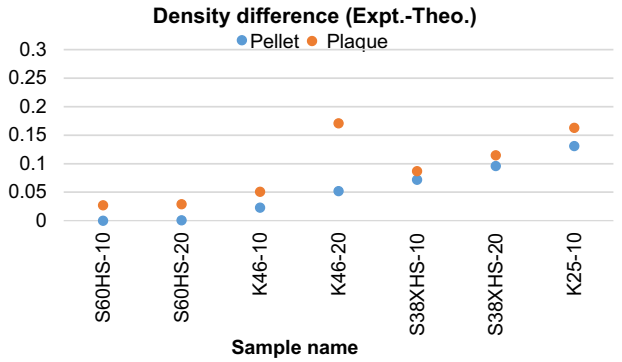

Figure 1. Plot of density differences (expt.-calc.) for the pellets and plaques.

The density calculations showed that the HGB underwent more breakage during the injection moulding process than during the compounding process and in all instances; the breakages were more for higher loadings of the filler. This was due to the higher applied shear stress during injection moulding. Additionally, the higher loading leads to higher volume fractions and the channels of the screw are fully filled which again leads to higher applied stress. However, based on the crush strengths of each grade, the extent of breakage varied. K25 showed the maximum breakage and S60HS showed the least breakage. This was in conformity with the crush strength values mentioned in table 1. The breakage of the HGB was qualitatively validated by SEM studies. The composites were charred and the residues, which are the HGB, were studied in SEM. The SEM images (figure 2a–d) are from the charred composites containing 10 wt% of the HGB, for each formulation. The images clearly depict that the S60HS grade (figure 2a) of HGB showed the least breakage and the K25 grade (figure 2d),

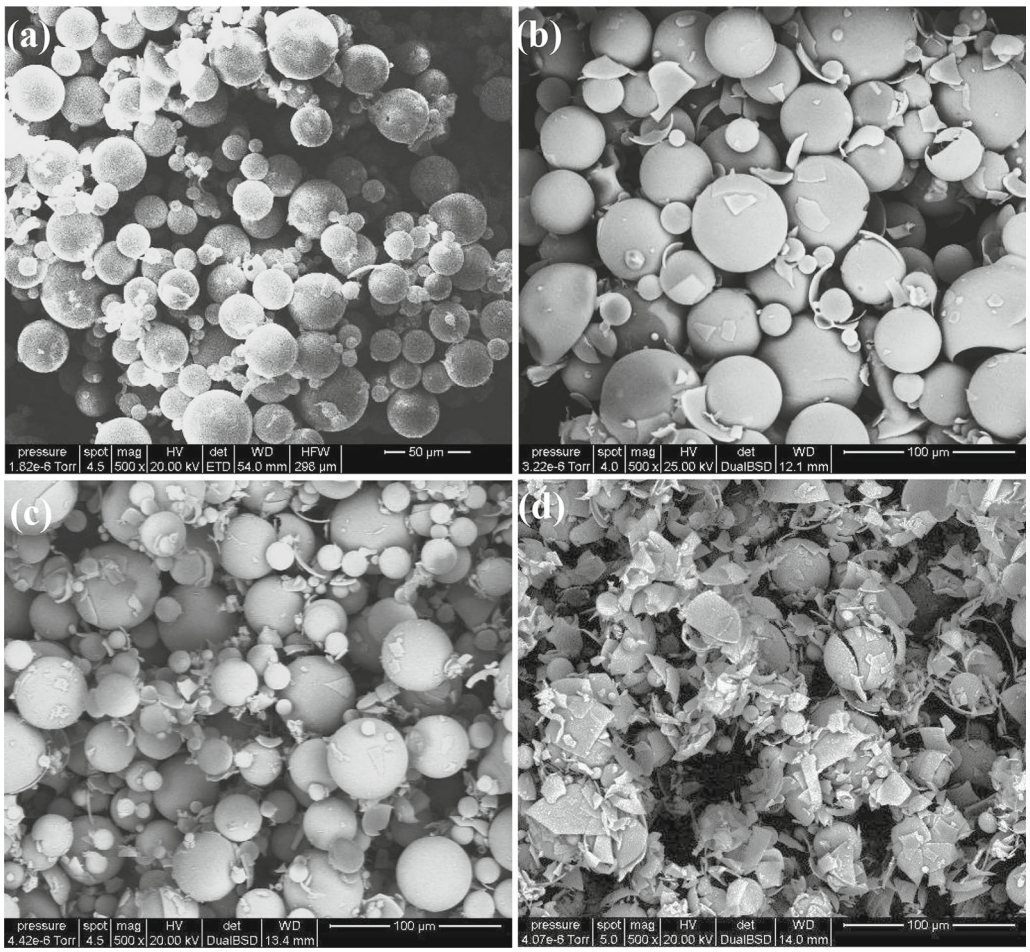

Figure 2. SEM images showing the HGB breakage for composite with (**a**) 10 wt% S60HS, (**b**) 10 wt% K46, (**c**) 10 wt% S38XHS and (**d**) 10 wt% K25.

Table 3. Experimental and calculated values of the thermal conductivities of the HGB-based composites plaques.

Moulded plaques	% loading of HGB	% char (actual % loading of HGB)	Thermal conductivity (expt. - λ_E) (W m^{-1} K^{-1})	Thermal conductivity (calculated - λ_c) (W m^{-1} K^{-1})
PPE/PA66			0.235	
S60HS-10	10	9.6	0.221	0.228
S60HS-20	20	18.7	0.222	0.223
K46-10	10	9.6	0.194	0.215
K46-20	20	18.2	0.221	0.2
S38XHS-10	10	7.7	0.214	0.208
S38XHS-20	20	16.2	0.194	0.18
K25-10	10	9.4	0.227	0.173

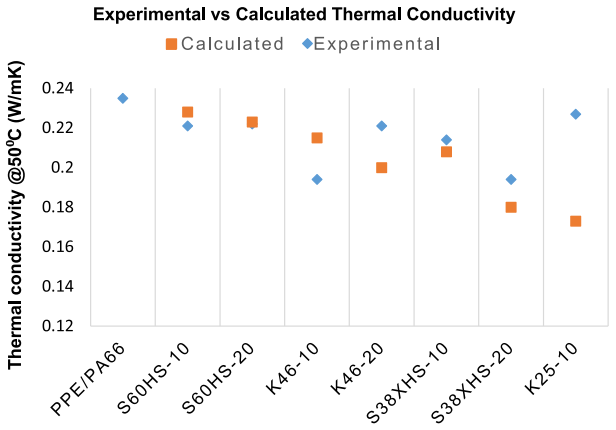

Figure 3. Graphical depiction of the experimental and calculated thermal conductivities of different samples.

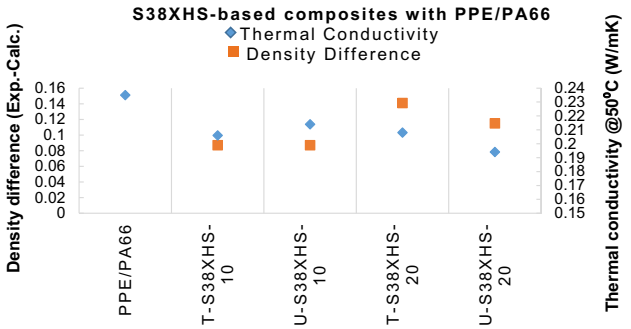

Figure 4. Plot of the density difference *vs.* thermal conductivity plot for S38XHS-based PPE/PA66 composites.

after moulding, had very few intact HGB. The other two grades had intermediate values.

The theoretical density calculation based on Nielsen's model was used to predict the thermal conductivity of the PPE/PA66 resin formulations containing HGB. It was observed that the model predicts value with good accuracy. The difference in predicted and experimentally measured values of thermal conductivity was attributed to the breakage of HGB. Table 3 shows the thermal conductivity values, both theoretical and experimental of the moulded plaques with 10 and 20 wt% of the HGB and figure 3 shows the plot of these thermal conductivity values of the moulded plaques.

From table 3, it is clear that the addition of higher strength HGB e.g., S60HS, irrespective of extent of loading, showed no reduction in the thermal conductivity of the PPE/PA composite. This is because initial thermal conductivity of S60HS is comparable to PPE/PA (refer table 1) due to higher glass content (higher shell thickness). Hence, though it did not break much during moulding, but it had minimal effect on the thermal conductivity of PPE/PA composite. On the other hand, inclusion of lower strength HGB e.g., K25 should have resulted in significant drop in thermal conductivity of PPE/PA composite as the thermal conductivity of K25 is much lower (refer table 1), but it was observed that effect was insignificant. This was due to the severe breakage of K25 into a glassy debris, rather than retaining its original hollow structure. Hence, effectively, there was no change in thermal conductivity at 10 wt% loading. Both for this reason and the fact that it was extremely fluffy material, higher loadings of K25 were not attempted. Addition of K46 and S38XHS led to significant reduction in thermal conductivity of PPE/PA which is due to the fact that thermal conductivity of these two HGB are low (refer table 1) and for these grades, there was less HGB breakage during moulding. Balance between the breakage and lower thermal conductivity/lower density of these HGB led to composites with reduced thermal conductivity as compared to the neat PPE/PA66 blend. The incorporation of the S38XHS grade of HGB showed the least difference in the extent of breakages at 10 and 20 wt% loadings and also fairly reduced thermal conductivities at higher loading. Hence, this grade of the HGB was chosen for further studies (figure 4).

A good interface between the HGB and the polymer matrix is important to achieve the lowest thermal

Table 4. Thermal conductivity and density difference calculations for S38XHS-based compositions.

Moulded plaques	% loading of HGB	% char (actual loading of HGB)	Thermal conductivity (expt. - λ_E) (W m^{-1} K^{-1})	$\rho_{plaque\ (diff)}$ ($\rho_{T2} - \rho_{E2}$)
PPE/PA66			0.235	
T-S38XHS-10	10	9	0.206	0.087
U-S38XHS-10	10	7.7	0.214	0.087
T-S38XHS-20	20	13.2	0.208	0.141
U-S38XHS-20	20	16.2	0.194	0.115

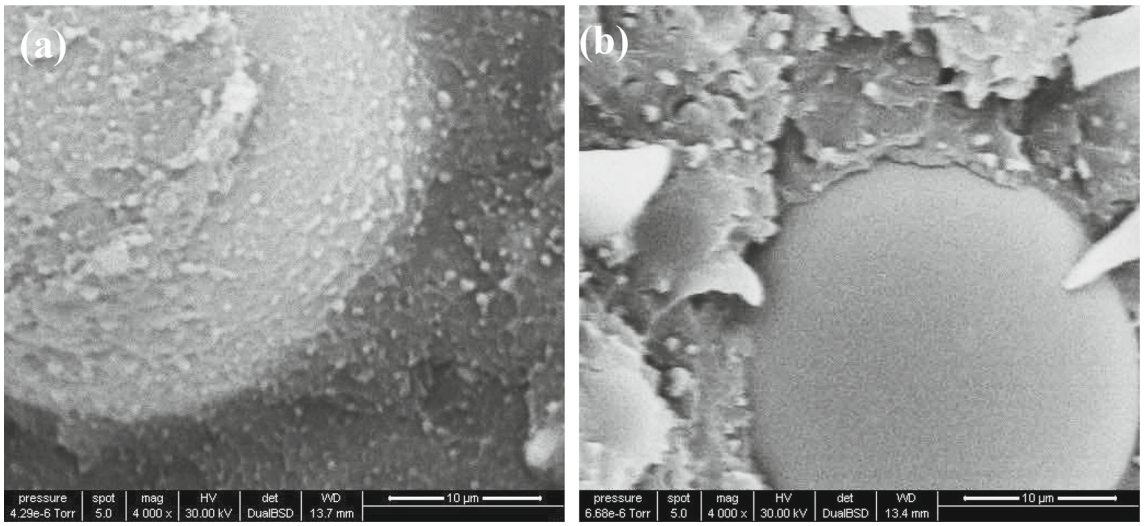

Figure 5. Representative SEM images of interfaces from PPE/PA66 composites using (**a**) surface-treated S38XHS and (**b**) untreated S38XHS grade of HGB.

conductivity [16] and balance of mechanicals, considering that the target application of these blends is in the area of building and construction. Few composite batches with surface treated (T) and untreated (U) HGB S38XHS grade were prepared and these compositions are mentioned as U-S38HS and T-S38HS, respectively. Table 4 shows the thermal conductivities of moulded plaques and density differences. The char values indicated the actual loading of HGB in the composite. These results endorsed the earlier observations. Overall, there was 20% reduction in thermal conductivity upon the addition of ~16 wt% of S38XHS in the PPE/PA66 resin formulation as compared to the neat PPE/PA66 resin. The treated HGB gave better wetting of the HGB with the polymer resin as compared to the untreated HGB. This is clearly visible in the SEM image of figure 5. The interface of the sample with surface-treated HGB grade is seamless, whereas the untreated HGB results in interfacial gaps, between the matrix and HGB. This resulted in improved mechanicals. For instance, in the 20 wt% compositions, i.e., U-S38HS-20 and T-S38HS-20, significant improvement was noticed with the treated HGB-based composites (T-S38HS-20) as compared to the batch with untreated S38HS. The tensile strength at break improved from 52 to 72 MPa; % strain at break increased from 2.7 to 5.2 and the heat deflection temperature (HDT) at 1.8 MPa strain showed a jump from 166 to 173°C. The details of these measurements are outlined elsewhere [15].

4. Conclusions

PPE/PA6 /HGB composites were prepared and thermal conductivity measurements were carried out on the injection-moulded plaques. These composites were expected to have lower thermal conductivities as compared to the neat PPE/PA66 resin, provided that the integrity of HGB remained intact during the compounding and moulding processes. However, the HGB fillers in these composites underwent breakage, both at compounding and moulding processes despite using optimized processing conditions. The breakage was estimated by density measurements on the pellets and moulded composite plaques. The extent of breakage was correlated with the density differences between the pellets and plaques, for each grade of HGB. SEM imaging of the HGB, extracted from the plaques by charring, validated the inter-dependencies of extent of breakage and thermal conductivity.

The thermal conductivities of the as-prepared composites were measured according to the guarded heat-flow method described in ASTM E1530-06. The corresponding theoretical conductivities of the composites were calculated using the Lewis and Nielsen's semi-theoretical model. These studies revealed that the thermal conductivity of the as-prepared composite plaques were a function of the factors, such as crush strength, density, wall thickness, etc. of HGB and polymer resin, the loadings of HGB, the breakage of HGB during processing, screw design and processing conditions. Of the tested HGB, S38XHS gave the optimum balance of thermal conductivity and crush strength, leading to $\sim$20% reduction in thermal conductivity as compared to neat PPE/PA66 resin.

Acknowledgements

We gratefully acknowledge the SABIC management for the opportunity to work on this project. We acknowledge Susanta Mitra and Narayana Rao for providing useful inputs and suggestions for summarizing the work.

References

[1] Zacha J, Hroudováb J, Brožovskýc J, Krejzad Z and Gailiuse A 2013 *Procedia Eng.* **57** 1288
[2] La Rosa A D, Recca A, Gagliano A, Summerscales J, Latteri A, Cozzo G *et al* 2014 *Construct. Build. Mater.* **55** 406
[3] Takagi H, Kako S, Kusano K and Ousaka A 2007 *Adv. Compos. Mater*. **16** 377
[4] Li X, Tabil L G, Oguocha I N and Panigrahi S 2008 *Compos. Sci. Technol*. **68** 1753
[5] Al-Homoud M S 2005 *Build Environ.* **40** 353
[6] Dittenber D B and Ganga Rao H V S 2012 *Composites Part A: Appl. Sci. Manuf.* **43** 1419
[7] Joshi S V, Drzal, L T, Mohanty A K and Arora S 2004 *Composites: Part A* **35** 371
[8] Abdou A and Budaiwi I 2013 *Construct. Build. Mater.* **43** 533
[9] Deepthi M V, Sharma M, Sailaja R R N, Anantha P, Sampathkumaran P and Seetharamu S 2010 *Mater. Des.* **31** 2051
[10] Alkadasi A N, Hundiwale D G and Kapadi U R 2004 *J. Appl. Polym. Sci*. **91** 1322
[11] Parvaiz M R, Mohanty S, Nayak S K and Mahanwar P A 2011 *Mater. Sci. Eng. A* **528** 4277
[12] Nechita P and Ionescu S M 2018 *J. Thermoplast. Compos. Mater.* **31** 1497
[13] Liang J Z 2000 *J. Macromol. Mater. Eng.* **287** 588
[14] Liang J Z and Li F H 2006 *Polym. Test* **25** 527
[15] Jha R K, Kamalakaran R, Mahanth S H and Narayan S 2010 (Innovative Plastics IP B.V.) US Patent 8617702B
[16] Liang J Z and Li F H 2007 *Polym. Test* **26** 419
[17] Nielsen L E 1974 *Ind. Eng. Chem. Fundam.* **13** 17
[18] Lewis T A and Nielsen L E 1970 *J. Appl. Polym. Sci.* **14** 1449